Permeability of Three-Dimensional Random Fiber Webs

A. Koponen,¹ D. Kandhai,² E. Hellén,³ M. Alava,^{3,4} A. Hoekstra,² M. Kataja,¹ K. Niskanen,⁵ P. Sloot,² and J. Timonen¹

¹Department of Physics, University of Jyväskylä, P.O. Box 35, FIN-40351 Jyväskylä, Finland

²Department of Mathematics, Computer Science, Physics and Astrophysics, University of Amsterdam,

³Laboratory of Physics, Helsinki University of Technology, P.O. Box 1100, FIN-02015, HUT, Finland

⁴Nordita, Blegdamsvej 17, DK-2100 Copenhagen, Denmark

⁵KCL Paper Science Center, P.O. Box 70, FIN-02151 Espoo, Finland

(Received 25 August 1997)

We report the results of essentially *ab initio* simulations of creeping flow through large threedimensional random fiber webs that closely resemble fibrous sheets such as paper and nonwoven fabrics. The computational scheme used in this Letter is that of the lattice-Boltzmann method and contains no free parameters concerning the properties of the porous medium or the dynamics of the flow. The computed permeability of the web is found to be in good agreement with experimental data, and confirms that permeability depends exponentially on porosity over a large range of porosity. [S0031-9007(97)05087-4]

PACS numbers: 47.55.Mh, 47.15.Gf

Fluid flow in porous media plays an important role in a wide variety of technical and environmental processes such as oil recovery, paper manufacturing, and spread of hazardous wastes in soils. The single-phase creeping flow through a porous substance in a gravitational field \mathbf{g} is well described by Darcy's law [1,2] which, in this case, can be written in a form

$$\mathbf{q} = \frac{k}{\nu} \,\mathbf{g}\,,\tag{1}$$

where **q** is the fluid flux through the medium, ν is the kinematic viscosity of the fluid, and *k* is the permeability coefficient that is a measure of the fluid conductivity through the porous medium.

Determination of coefficient k for each particular substance has been a long-standing problem. The experimental methods that have been used to this end vary from rather straightforward measurements [3–5] to more sophisticated approaches, which utilize, e.g., mercury porosimetry, electrical conductivity, nuclear magnetic resonance, or acoustic properties of the medium [6]. Theoretical methods typically rely on analytical models based on simplified pore geometries, which allow solution of the microscopic flow patterns [1], or on more advanced methods that statistically take into account the structural complexity of the medium [1,2].

Numerical simulations are often used to connect theory with experiments. Realistic three-dimensional flow simulations in complex geometries are, however, very demanding in terms of computing power. Until recently this approach has thus been hampered by the necessity of major simplifications in the pore structure or flow dynamics. New techniques based on massively parallel computers and increased single processor capabilities have now made 3D *ab initio* simulations of realistic flow problems feasible. This development is further augmented by the recent introduction of new flow-simulation algorithms that are particularly suited for parallel computing. Among these are the lattice-gas-automaton [7,8] and lattice-Boltzmann method [9–11], which have already been applied to a wide class of fluid-flow problems. These methods are particularly useful in complex and irregular geometries [12–16].

Despite the numerous experimental and theoretical studies (see, e.g., [5] for a comprehensive review), permeability characteristics of disordered fibrous porous media are still poorly understood. The existing numerical studies include those on fluid flow through random arrays of parallel cylinders, suspension of prolate spheroids, and threedimensional regular fiber networks, which all neglect the disorder typical of real 3D fiber webs [17-19].

In this Letter we report the results of three-dimensional lattice-Boltzmann simulations of creeping flow through large random fiber webs, and compare these results with previous experimental, analytical, and numerical results for various fibrous materials.

The model web structures were constructed in discretized space using a recently introduced growth algorithm [20]. Within this algorithm, fiber webs are grown by sequential random deposition of flexible fibers of rectangular cross section on top of a flat substrate (the xyplane). Each fiber was randomly oriented either in the xor y direction, and was then let to fall in the negative zdirection until it made its first contact with the underlying structure. After this it was bent downwards without destructing the structure, and subject to the constraint

$$|z_i - z_j| \le F. \tag{2}$$

Here z_i and z_j are the elevations of the fiber surface above two nearest-neighbor cells *i* and *j*, and *F* is an effective fiber flexibility. Notice that for long fibers, the resulting

Kruislaan 403, NL-1098 SJ Amsterdam, The Netherlands

web structure, porosity, and contact area of fibers depend only on F [21]. A large F produces a dense web while a small F leads to a more porous structure.

In order to construct structures that are homogeneous in the z direction, the samples used in the simulations were extracted from inside of thicker webs. Ten grid layers of void space were then added on the top of samples, and the system was made periodic in all directions. In Fig. 1 we show a sample created by this algorithm. It is evident that the produced structures closely resemble those of, e.g., paper [22] and nonwoven fabrics (restriction to the x and y directions can be relaxed and does not play an important role here).

Simulations of fluid flow through the web in the z direction were done using the 19-link LBGK (lattice-Bhatnagar-Gross-Krook) model [9]. Flow was induced by applying a "gravitational" body force on the fluid [14]. This was accomplished simply by adding at each time step a fixed amount of momentum in the negative z direction to all "particles" within the pore space. In Fig. 2 we show the simulated stationary velocity field for a flow in the z direction through the highly inhomogeneous sample shown in Fig. 1.

It is evident that there are large fluctuations in the velocity field reflecting the variations in the local porosity of the sample. The average velocity $\langle v_z \rangle$ shown in Fig. 2 is $\langle v_z \rangle = 0.00142$ (in grid units), with a standard deviation of $\Delta v_z = 0.00128$. These fluctuations, which are inherent in random porous structures, will affect the permeability, except at very high porosities, such that it is expected to become higher than that for regular arrays of pores [5]. This effect will be seen in the results given below.

In a stationary state the body force applied to the fluid is completely canceled by viscous friction forces due to fibers. Once the total flux of fluid through the sample and the viscosity of the fluid are known, the permeability of the sample can then be determined from Darcy's law Eq. (1). It is well known that the permeability of a porous medium determined by the present method depends on grid resolution. Resolution sensitivity is caused by the bounce-back boundary condition applied to the solid-fluid interface, and by Knudsen effects in small pores [8,11,14]. These effects are viscosity dependent, and they determine the minimum size of obstacles and pores that can be used in simulations.

In order to find an acceptable grid resolution in different porosity regions, we first made a series of test runs using fibers of aspect ratio 10, i.e., of size $w_F \times w_F \times 10w_F$, with $w_F = 5$, 10, and 20 grid units. In these tests the size of the simulation sample was $L_x \times L_y \times L_z =$ $20w_F \times 20w_F \times 10w_F$. The relaxation parameter τ of the LBGK collision operator was varied from 0.668 to 2 corresponding to the dynamic viscosity $\nu = (2\tau - 1)/6$ [9] ranging from 0.056 to 0.5 (in grid units).

In Fig. 3 we show the computed permeability as a function of viscosity ν for two test systems of different porosities. The nearly linear dependence on ν of permeability [14] is clearly seen in this figure. For $\phi = 0.67$ [Fig. 3(a)], the result is already almost independent of the grid resolution for the smallest value of viscosity. For high porosities ϕ (with $\nu = 0.056$), resolution $w_f = 5$ can thus be used. For a smaller ϕ finite-size effects become more pronounced. Comparing the simulated permeabilities for $\phi = 0.39$ [Fig. 3(b)] at $\nu = 0.056$, we can conclude that $w_F = 10$ is satisfactory for low porosities.

In the actual permeability simulations fibers of aspect ratio 20, i.e., of size $w_F \times w_F \times 20w_F$, and a sample of dimensions $80w_F \times 80w_F \times 10w_F$ were used. (In Fig. 1 we show an example of the webs for which simulations were performed.) The flexibility parameter *F* was varied from 0 to 3 which corresponds to porosities ϕ ranging from 0.95 to 0.42. In the simulations $\tau = 0.668$ ($\nu = 0.056$) and two different values for w_F were used. For $\phi > 0.6$, $w_F = 5$ was used, and the size of the simulation lattice was $400 \times 400 \times 60$ grid points. For $\phi < 0.6$, $w_F = 10$ and a lattice of $800 \times 800 \times 110$ grid points were used. For these discretizations, the

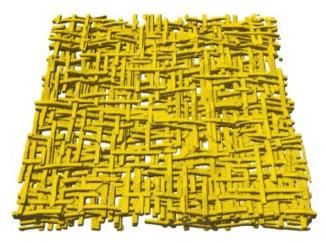


FIG. 1(color). A fiber-web sample constructed with the deposition model. The porosity of the web is 0.83.

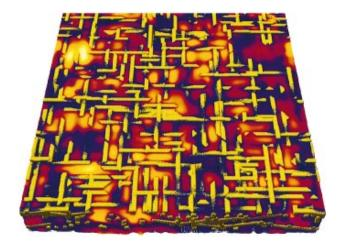


FIG. 2(color). The velocity field of fluid flow through the fiber web shown in Fig. 1. Bright colors indicate high fluid velocity.

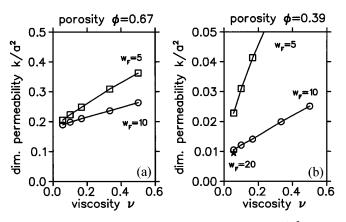


FIG. 3. Calculated dimensionless permeability k/a^2 as a function of viscosity ν for two test samples with porosities (a) $\phi = 0.67$ and (b) $\phi = 0.39$. Here $a = w_F/2$ is the hydraulic radius of the fibers. The fiber widths (grid resolutions) are $w_F = 5$ (squares), 10 (circles), and 20 (star).

estimated finite-size errors of the simulated permeabilities were less than 15%.

Simple dimensional analysis suggests that, for a constant body force, the saturation time for reaching the steady state is proportional to R_{pore}^2/ν , where R_{pore} is the characteristic size of pores. For systems with high porosity, saturation time thus tends to become very long. This time can, however, be essentially reduced by using an iterative momentum relaxation (IMR) method in which the applied body force is changed during simulation depending on the value of the friction force. A thorough description of the IMR method and a detailed benchmark analysis of our parallel lattice-Boltzmann code will be published separately [23,24]. In the IMR method the number of time steps required for saturation (with 1% accuracy) varied between 1000 to 8000 depending on porosity, and was typically less than half of that needed in the constantbody-force method. When 32-bit floating point numbers were used, the larger simulation lattice required 5.4 Gbyte of core memory. The simulations were therefore carried out using 64 nodes (300 MHz CPUs with 128 Mbyte of memory) on a Cray T3E system. The required CPU time was typically between 1 and 4 hours.

In Fig. 4 we show the simulated permeability of the random fiber web as a function of its porosity. In this figure solid triangles denote the simulated values: the related porosities were given by the flexibility parameter (F) used. It is evident that there are two distinct features in the simulated $k(\phi)$ curve. First, it seems to diverge as expected when $\phi \rightarrow 1$, and, second, k seems to be an exponential function of ϕ for a rather wide range of ϕ : $0.42 \leq \phi \leq 0.85$.

A fit to the last five points with highest porosities of the form $k/a^2 = \text{const} \times (1 - \phi)^{-\mu}$ gives $\mu = 1.92$. This result shows that even for these rather high porosities $\phi \leq 0.96$, the system is not in the true asymptotic region for which $\mu = 1$ [25]. The reason for this is that the fibers of the web are still close enough to each other

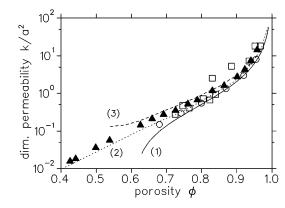


FIG. 4. The calculated dimensionless permeability k/a^2 as a function of porosity (black triangles). Open squares and circles show the experimental results for fibrous filters [5] and compressed fiber mats [3,5], respectively. Curve (1) is the analytical result for cubic lattice given in Ref. [5], curve (2) is the numerical result for an fcc lattice from Ref. [19], and curve (3) shows the result of a fit with the Kozeny-Carman relation, Eq. (3).

so that there are significant hydrodynamic interactions between them. On the other hand, the simple capillarytube model by Kozeny and Carman [1] gives $k/a^2 \propto \phi^3(1-\phi)^{-2}$ in this limit so that, as expected, the simulated behavior of $k(\phi)$ is rather in good agreement with this model when $\phi \leq 1$.

A fit of the form $\ln(k/a^2) = A + B\phi$ to the rest of the simulated points gives A = -8.53, B = 10.4, with a very high correlation between the simulated points and the fitted curve. So far there have been no analytical results which would have produced this kind of exponential behavior at intermediate porosities. It will not hold near the percolation threshold at which permeability vanishes. This critical region is, however, beyond the present computational capabilities.

Experimental results [3,5], shown in Fig. 4 as open circles and squares, conform well with the simulated points. Notice that there is no free parameter in the present model as permeability is scaled by the square of the hydraulic radius of the fibers, and the relaxation parameter τ is used only to fix the necessary grid resolution. The level of agreement is therefore astonishingly high. It also shows that the model web used here captures the essential features of the fibrous filters and compressed fiber mats used in the experiments.

Also shown in Fig. 4 are three curves which are results of previous analytical [5] [curve (1)], numerical [19] [curve (2)], and semiempirical [1,3,4] [curve (3)] considerations. Curve (1) is given by $k/a^2 = -\ln(1 - \phi) - 0.931$ [with $O(1/\ln(1 - \phi))$], an expression obtained [5] for a cubic lattice model, and curve (2) results from a numerical solution [19] for the Stokes flow in a face-centered-cubic (fcc) array of fibers. Both these curves are below the simulated points, especially for decreasing porosity. Notice that the fcc result also follows an exponential law at intermediate porosities. It is

30%-40% below the random fiber-web result for these porosities, but approaches the latter for small porosities since the percolation threshold of the fcc lattice [19] is at a much lower porosity.

Curve (3) is the Kozeny-Carman expression [1]

$$k = \phi^3 / cS^2, \tag{3}$$

where *S* is the specific surface area of the web, and *c* is a constant in capillary-tube models but is known to depend on porosity in fibrous materials [4]. An empirical fit to measured porosities of these materials gives [3,4] $c = 3.5\phi^3[1 + 57(1 - \phi)^3]/(1 - \phi)^{\frac{1}{2}}$, and we have used this expression to get the curve (3) from Eq. (3). The specific surface area *S* was determined from the surface area of the (straight) fibers used to construct the web by subtracting the area of the interfiber contacts. Because of bending of the fibers this expression gives a lower bound for *S*, and curve (3) is expected to overestimate the permeability. This is indeed what happens (cf. Fig. 4).

Encouraged by the exponential behavior at intermediate porosities of $k(\phi)$, we have made an interpolation formula that connects this behavior with the right asymptotics in the limit $\phi \rightarrow 1$. We find that the expression $k/a^2 =$ $A[e^{B(1-\phi)} - 1]^{-1}$ with A = 5.55, B = 10.1 fits all the simulated points very well. So far we have no theoretical arguments to support this very simple form for the permeability.

In conclusion, we used the lattice-Boltzmann method on a massively parallel computer to solve *ab initio* the permeability of a large random 3D fiber web as a function of its porosity in a large porosity range. An iterative momentum relaxation method was used to considerably reduce the computing time needed for reaching stationary flows. The web samples used were constructed by a growth algorithm [20] that produces random structures of flexible fibers, closely resembling those of, e.g., paper sheets and nonwoven fabrics. The simulated results were found to be in excellent agreement with experiments on the materials mentioned above. There were no free parameters in the simulations which would have been used for fitting with the experimental results, and also in this sense the results reported are *ab initio*. We found that the exponential dependence on porosity of permeability in a wide range of porosities is a generic feature of fibrous porous materials, independent of whether they are random or not. So far there is no theoretical explanation for this phenomenon, but a simple interpolation expression for $k(\phi)$ was formulated which seems to give the correct behavior in the whole range of porosities above the critical region near the percolation threshold. The results reported here clearly demonstrate that ab initio simulations of flow in complicated structures are possible (see also Refs. [14,15]), and many open problems in this area can and will now be addressed.

We thank the Center for Scientific Computing in Finland (Sami Saarinen and Tomi Salminen in particular) for providing computational resources, technical support, and expertise on visualization.

- [1] J. Bear, *Dynamics of Fluids in Porous Media* (Dover, New York, 1972).
- [2] M. Sahimi, Flow and Transport in Porous Media and Fractured Rock (VCH, Weinheim, 1995).
- [3] W.L. Ingmanson, B.D. Andrews, and R.C. Johnson, Tappi 42, 840 (1959).
- [4] S. T. Han, Pulp Pap. Mag. Can. 70, T134 (1969).
- [5] G.W. Jackson and D.F. James, Can. J. Chem. Eng. 64, 364 (1986).
- [6] See S. Kostek, L. M. Schwartz, and D. L. Johnson, Phys. Rev. B 45, 186 (1992); A. H. Thompson, S. W. Sinton, S. L. Huff, A. J. Katz, R. A. Raschke, and G. A. Gist, J. Appl. Phys. 65, 3259 (1989); D. L. Johnson, D. L. Hemmick, and H. Kojima, J. Appl. Phys. 76, 104 (1994), and references therein.
- [7] U. Frisch, D. d'Humiéres, B. Hasslacher, P. Lallemand, Y. Pomeau, and J.-P. Rivet, Complex Syst. 1, 649 (1987).
- [8] D. H. Rothman and S. Zaleski, *Lattice Gas Cellular Automata* (Cambridge University Press, Cambridge, England, 1997).
- [9] Y. H. Qian, D. d'Humiéres, and P. Lallemand, Europhys. Lett. 17, 479 (1992).
- [10] R. Benzi, S. Succi, and M. Vergassola, Phys. Rep. 222, 145 (1992).
- [11] I. Ginzbourg and D. d'Humiéres, J. Stat. Phys. 84, 927 (1996).
- [12] A. Cancelliere, C. Chang, E. Foti, D.H. Rothman, and S. Succi, Phys. Fluids A 2, 2085 (1990).
- [13] A.J.C. Ladd, J. Fluid Mech. 271, 285 (1994); A.J.C. Ladd, J. Fluid Mech. 271, 311 (1994).
- [14] B. Ferréol and D. H. Rothman, Transp. Porous Media 20, 3 (1995).
- [15] N.S. Martys and H. Chen, Phys. Rev. E 53, 743 (1996).
- [16] J. Kaandorp, C. Lowe, D. Frenkel, and P. Sloot, Phys. Rev. Lett. 77, 2328 (1996).
- [17] C.K. Ghaddar, Phys. Fluids 7, 2563 (1995).
- [18] I.L. Clayes and J.F. Brady, J. Fluid Mech. 251, 443 (1993).
- [19] J. J. L. Higdon and G. D. Ford, J. Fluid Mech. 308, 341 (1996).
- [20] K. Niskanen and M. Alava, Phys. Rev. Lett. 73, 3475 (1994).
- [21] E. K. O. Hellén, M. J. Alava, and K. J. Niskanen, J. Appl. Phys. 81, 6425 (1997).
- [22] K. Niskanen, N. Nilsen, E. Hellén, and M. Alava, in *The Fundamentals of Papermaking Materials*, edited by C. F. Baker (Pira Int., Leatherhead, UK, 1997).
- [23] D. Kandhai, A. Koponen, A. Hoekstra, M. Kataja, J. Timonen, and P. Sloot (to be published).
- [24] D. Kandhai, A. Koponen, A. Hoekstra, M. Kataja, J. Timonen, and P. Sloot, Comput. Phys. Commun. (to be published).
- [25] G.K. Bachelor, J. Fluid Mech. 52, 245 (1972).